BJ www.biochemj.org

BJ Disease

Biochem. J. (2011) **437**, 443–453 (Printed in Great Britain) doi:10.1042/BJ20110510

Metabolic oxidative stress elicited by the copper(II) complex [Cu(isaepy)$_2$] triggers apoptosis in SH-SY5Y cells through the induction of the AMP-activated protein kinase/p38^{MAPK}/p53 signalling axis: evidence for a combined use with 3-bromopyruvate in neuroblastoma treatment

Giuseppe FILOMENI*[1], Simone CARDACI*[1], Ana Maria DA COSTA FERREIRA†, Giuseppe ROTILIO*‡ and Maria Rosa CIRIOLO*‡[2]

*Department of Biology, University of Rome "Tor Vergata", via della Ricerca Scientifica, 00133 Rome, Italy, †Departamento de Química Fundamental, Instituto de Química, Universidade de São Paulo, Av. Prof. Lineu Prestes 748, CEP 05508-900, São Paulo, SP, Brazil, and ‡Research Centre IRCCS San Raffaele Pisana, Via dei Bonacolsi, 00163 Rome, Italy

We have demonstrated previously that the complex bis[(2-oxindol-3-ylimino)-2-(2-aminoethyl)pyridine-*N*,*N*′]copper(II), named [Cu(isaepy)$_2$], induces AMPK (AMP-activated protein kinase)-dependent/p53-mediated apoptosis in tumour cells by targeting mitochondria. In the present study, we found that p38^{MAPK} (p38 mitogen-activated protein kinase) is the molecular link in the phosphorylation cascade connecting AMPK to p53. Transfection of SH-SY5Y cells with a dominant-negative mutant of AMPK resulted in a decrease in apoptosis and a significant reduction in phospho-active p38^{MAPK} and p53. Similarly, reverse genetics of p38^{MAPK} yielded a reduction in p53 and a decrease in the extent of apoptosis, confirming an exclusive hierarchy of activation that proceeds via AMPK/p38^{MAPK}/p53. Fuel supplies counteracted [Cu(isaepy)$_2$]-induced apoptosis and AMPK/p38^{MAPK}/p53 activation, with glucose being the most effective, suggesting a role for energetic imbalance in [Cu(isaepy)$_2$] toxicity. Co-administration of 3BrPA (3-bromopyruvate), a well-known inhibitor of glycolysis, and succinate dehydrogenase, enhanced apoptosis and AMPK/p38^{MAPK}/p53 signalling pathway activation. Under these conditions, no toxic effect was observed in SOD (superoxide dismutase)-overexpressing SH-SY5Y cells or in PCNs (primary cortical neurons), which are, conversely, sensitized to the combined treatment with [Cu(isaepy)$_2$] and 3BrPA only if grown in low-glucose medium or incubated with the glucose-6-phosphate dehydrogenase inhibitor dehydroepiandrosterone. Overall, the results suggest that NADPH deriving from the pentose phosphate pathway contributes to PCN resistance to [Cu(isaepy)$_2$] toxicity and propose its employment in combination with 3BrPA as possible tool for cancer treatment.

Key words: AMP-activated protein kinase (AMPK), 3-bromopyruvate, delocalized lipophilic cation, neuroblastoma, p38 mitogen-activated protein kinase (p38^{MAPK}), p53.

INTRODUCTION

AMPK (AMP-activated protein kinase) is a heterotrimeric serine/threonine protein kinase which acts as a fuel sensor in eukaryotic cells [1]. It is activated physiologically when the AMP/ATP ratio increases and mediates the phosphorylation of a large number of metabolic enzymes aimed at the restoration of ATP levels. However, AMPK activation is enhanced under stress conditions associated with energetic imbalance, such as glucose deprivation, hypoxia and the production of ROS (reactive oxygen species) [1–3]. Besides energy balance control, previous findings have highlighted that AMPK-driven phosphorylation cascades can produce antiproliferative effects in response to a variety of insults by inhibiting cell growth, slowing down cell-cycle progression and promoting apoptosis [4–6]. Although AMPK-mediated cell growth inhibition mainly depends on the suppression of mTOR (mammalian target of rapamycin) activity, which limits protein synthesis and activates autophagy [4,7], cell-cycle arrest and the induction of apoptosis seem to rely, at least in part, on p53 activation [8,9]. AMPK-mediated p53 phospho-activation plays a crucial role either in the glucose-dependent regulation of a G_1/S metabolic checkpoint [10] or in the induction of apoptosis elicited by severe carbon source depletion and genotoxic stresses [8,11]. Other pieces of evidence indicate that AMPK can also affect cell proliferation by the induction of apoptosis via the MAPK (mitogen-activated protein kinase) pathway, mainly those dependent on p38^{MAPK} and JNK (c-Jun N-terminal kinase). The former mediates the pro-apoptotic activity of AMPK upon UV and H_2O_2 exposure [8], with the latter being phospho-activated upon exposure to cannabinoid antagonists and under conditions of sustained AMPK activation [12,13]. Overall, these findings suggest that AMPK can be considered a molecular target for a feasible therapeutic strategy in cancer. Consistent with these observations, during the last few years, novel chemotherapeutics have been developed to selectively affect tumour growth and viability by promoting AMPK activation. For instance, several antidiabetic drugs, such as metformin and the thienopyridone A769662, delay the growth of spontaneous tumours in an AMPK-responsive manner [12–15]. Moreover, evidence that PIAs (phosphatidylinositol ether

Abbreviations used: AMPK, AMP-activated protein kinase; 3BrPA, 3-bromopyruvate; [Cu(isaepy)$_2$], bis[(2-oxindol-3-ylimino)-2-(2-aminoethyl)pyridine-*N*,*N*′]copper(II); DCF, dichlorodihydrofluorescein; DCFH-DA, 2′,7′-dichlorodihydrofluorescein diacetate; DHEA, dihydroepiandrosterone; DLC, delocalized lipophilic cation; D/N, dominant-negative; 2,4-DNPH, 2,4-dinitrophenylhydrazine; DQC, dequalinium chloride; FBS, fetal bovine serum; GAPDH, glyceraldehyde-3-phosphate dehydrogenase; KM, kinase mutant; MAPK, mitogen-activated protein kinase; 2-NBDG {2-[*N*-(7-nitrobenz-2-oxa-1,3-diazol-4-yl) amino]-2-deoxy-D-glucose; PCN, primary cortical neuron; RA, retinoic acid; Rho123, rhodamine 123; ROS, reactive oxygen species; siRNA, small interfering RNA; SOD1, superoxide dismutase 1; WT, wild-type.

[1] These authors contributed equally to the study.

[2] To whom correspondence should be addressed (email ciriolo@bio.uniroma2.it).

lipid analogues) and some natural compounds, such as curcumin and selenium, are able to elicit apoptosis in various cancer cell lines by activating AMPK [16–18] strengthens the idea that this kinase can represent a promising target both for anticancer and chemopreventive drugs.

Several studies have demonstrated that cancer cells undergo a complex metabolic and bioenergetic reprogramming aimed at sustaining a higher rate of growth and proliferation. This biochemical reorganization mainly consists of an increase in the glycolytic rate under normal oxygen tension (aerobic glycolysis or the 'Warburg effect'), which allows tumour cells to use large amounts of glucose as carbon source for anabolic reactions [3,19] and to survive under restrictive conditions [19,20]. In accordance with this feature, ATP-depleting molecules, such as the glycolytic inhibitors 2-deoxyglucose [21] and 3BrPA (3-bromopyruvate) [22], as well as several compounds able to affect oxidative phosphorylation, have been exploited as tumour cell death inducers. Among them, DLCs (delocalized lipophilic cations), such as Rho123 (rhodamine 123), the thiopyrilium AA-1 and DQC (dequalinium chloride), owing to their ability to selectively target mitochondria [23], are considered an efficient class of chemotherapeutics.

One chemotherapeutic strategy is to combine two or more drugs that affect the metabolic activity of cancer cells at low doses in order to enhance their own killing properties and reduce the side effects on untrasformed healthy cells. For instance, the observation that many glycolytic inhibitors are able to improve the anticancer properties of several chemotherapeutics, including alkylating molecules [24], DNA-intercalating agents [25] and DLCs [26,27], reinforces the feasibility to develop novel anticancer therapies able to induce metabolic oxidative stress to overcome drug resistance and reduce systemic toxicity.

We have characterized previously the pro-apoptotic activity of bis[(2-oxindol-3-ylimino)-2-(2-aminoethyl)pyridine-*N*,*N*′]copper(II), named [Cu(isaepy)$_2$], an isatin–Schiff base copper(II) complex highly efficient in inducing neuroblastoma and carcinoma cell death [28,29]. We have demonstrated that [Cu(isaepy)$_2$] behaves as an uncoupler and a DLC-like molecule that yields oxidative damage in the mitochondrial compartment. In the present study, we have dissected the signalling pathways responsible for the final induction of [Cu(isaepy)$_2$]-induced apoptosis in SH-SY5Y cells, highlighting the role of the energetic-stress-responsive pathway AMPK/p38^{MAPK}/p53 as the principal route governing the apoptotic response. In addition, we have provided evidence supporting the putative use of this copper-based complex in combination with 3BrPA as a feasible therapeutic strategy for neuroblastoma treatment.

MATERIALS AND METHODS

Materials

The isatin–di-imine copper(II) complex [Cu(isaepy)$_2$](ClO$_4$)$_2$ {simply referred to as [Cu(isaepy)$_2$]}, was synthesized as described previously [28,30]. 3BrPA, DHEA (dihydroepiandrosterone), DMSO, DTT (dithiothreitol), glucose, methyl succinate, paraformaldehyde, propidium iodide, RA (retinoic acid), Rho123, sodium pyruvate and Triton X-100 were from Sigma. DQC was from Alexis. DCFH-DA (2′,7′-dichlorodihydrofluorescein diacetate) and 2-NBDG {2-[*N*-(7-nitrobenz-2-oxa-1,3-diazol-4-yl) amino]-2-deoxy-D-glucose} were from Alexis. The HRP (horseradish peroxidase)-conjugated goat anti-[mouse IgG (H + L)] antibody was from Bio-Rad Laboratories. Tes was from US Biological. All other chemicals were from Merck.

SH-SY5Y cells cultures

Human neuroblastoma SH-SY5Y cells were grown in DMEM (Dulbecco's modified Eagle's medium)/F12 supplemented with 10 % FBS (fetal bovine serum), glutamine and penicillin/streptomycin, and cultured at 37 °C in an atmosphere of 5 % CO_2 in air. During the experiments, cells were plated at a density of 4×10^4/cm^2, unless otherwise indicated. SH-SY5Y cells overexpressing the WT (wild-type) form of human SOD1 (superoxide dismutase 1) (*h*SOD cells) were obtained as described previously [28].

Mouse PCNs (primary cortical neurons)

Mouse PCNs were obtained from cerebral cortices of E15 (embryonic day 15) C57BL-6 mice embryos. All of the experiments were performed according to the Animal Research Guidelines of the European Communities Council Directive (86/609/EEC). Minced cortices were digested with 0.25 % trypsin (Lonza)/EDTA at 37 °C for 7 min. Cells were stained with 0.08 % Trypan Blue solution, and only viable cells were counted and plated at a density of 10^5/cm^2 on to poly-D-lysine-coated coverlips or multiwell plates in 5 mM (low glucose) or 25 mM glucose-containing MEM (minimal essential medium) supplemented with 10 % FBS, 2 mM glutamine and 0.1 mg/ml gentamicin (Invitrogen). After 1 h, the medium was replaced with Neurobasal medium containing antioxidant-free B27 supplement (Invitrogen), 2 mM glutamine and 0.1 mg/ml gentamicin. Cell cultures were kept at 37 °C in a humidified atmosphere containing 5 % CO_2. Every 3 days, one-third of the medium was replaced up to day 7, the time at which the cells were treated.

Transfections

At 24 h after plating, 50 % confluent SH-SY5Y cells were transfected with a SignalSilence® Pool p38^{MAPK} siRNA (sip38$_1$) (Cell Signaling Technology) or with a ON-TARGET*plus* p38^{MAPK} siRNA (sip38$_2$; Dharmacon, Thermo Fisher Scientific). Control cells were transfected with a scrambled siRNA (small interfering RNA) duplex (siScr), which does not have homology with any other human mRNAs. Overexpression of mutated proteins was carried out by transfecting the cells with a pcDNA3 empty vector or with a pcDNA3 vector containing: (i) the Myc-tagged coding sequence for the α2 subunit of AMPK carrying the T→A substitution at residue 172 (kindly provided by Professor David Carling, Clinical Sciences Centre, Imperial College, Hammersmith Hospital, London, U.K.); (ii) the FLAG-tagged coding sequence for the α1 subunit of p38^{MAPK} carrying a loss-of-function mutation in the catalytic residues [KM (kinase mutant); kindly provided by Professor Jiahuai Han, Department of Immunology, The Scripps Research Institute, La Jolla, CA, U.S.A.]. After transfection, cells were immediately seeded into fresh medium and used after 48 h, because this time was sufficient to significantly increase the expression of these D/N (dominant-negative) forms of the proteins. Cells were transfected by electroporation using a Gene Pulser Xcell system (Bio-Rad Laboratories), according to the manufacturer's instructions, and were seeded directly into fresh medium. Transfection efficiency was estimated by co-transfecting siRNA or plasmids with non-specific rhodamine-conjugated oligonucleotides and was found to be > 80 %.

Treatments

A 5 mM solution of [Cu(isaepy)$_2$] was prepared just before the experiments by dissolving the freeze-dried compounds in DMSO.

Treatments were performed in serum-supplemented medium with [Cu(isaepy)$_2$] at a final concentration of 50 μM, unless otherwise stated. DQC and Rho123 were dissolved in PBS and DMSO respectively and were used at 100 μM. The p53 inhibitor pifithrin-α was dissolved in DMSO and used at 20 μM. Fuel supplies were dissolved in PBS and added to the medium to reach a final concentration of 30 mM glucose, 10 mM sodium pyruvate or 10 mM methyl succinate. The glucose-6-phosphate dehydrogenase inhibitor DHEA was dissolved in DMSO and administered at a final concentration of 1 μM. 3BrPA was dissolved in PBS and used alone or in combination with [Cu(isaepy)$_2$] at 10 μM. RA was dissolved in DMSO and used at 20 μM in order to induce the differentiation of SH-SY5Y cells and was routinely re-added for a 2 week period. All of the treatments were maintained throughout the addition with [Cu(isaepy)$_2$]. As a control, equal volumes of PBS (for DQC, 3BrPA and fuel supplies) or DMSO (for the remaining compounds) were added to cell medium.

Cell viability

Cell viability was estimated by direct counting upon Trypan Blue exclusion. For the evaluation of apoptosis, cells were stained with 50 μg/ml propidium iodide prior to analysis using a FACScalibur instrument (BD Biosciences). The percentage of apoptotic cells was evaluated as described previously [31].

Measurement of ROS and carbonylated protein levels

Detection of intracellular ROS and protein carbonyls was performed as described previously [28]. Briefly, cells were incubated with 50 μM DCFH-DA (dissolved in DMSO) for 2 h at 37 °C, then treated with [Cu(isaepy)$_2$] and the fluorescence of DCF (dichlorofluorescein), generated upon the reaction with ROS, was analysed cytofluorimetrically. Treatment with 100 μM t-BOOH (t-butyl hydroperoxide) was used as a positive control. Carbonylated proteins were detected using the Oxyblot Kit (Intergen) after reacting with 2,4-DNPH (2,4-dinitrophenylhydrazine) for 15 min at 25 °C. Samples were resolved by SDS/PAGE (12 % gels) and 2,4-DNPH-derivatized proteins were identified by immunoblotting using an anti-2,4-DNPH antibody.

Measurement of 2-NBDG uptake

Cells were incubated for 1 h with 100 μM 2-NBDG (dissolved in DMSO), a fluorescent derivative of 2-deoxy-D-glucose, washed with PBS, collected and analysed cytofluorimetrically [32].

Extracellular lactate assay

Extracellular lactate concentration was assessed as described previously [33]. Briefly, 10 μl of trichloroacetic acid-precipitated proteins from cell medium was incubated at room temperature (25 °C) in 290 μl of a 0.2 M glycine/hydrazine buffer, pH 9.2, containing 0.6 mg/ml NAD^+ and 17 units/ml lactate dehydrogenase. NAD^+ reduction was followed at 340 nm and nmol of NADH formed were considered to be stoichiometrically equivalent to extracellular lactate.

Western blot analyses

Total lysates and mitochondrial enriched fraction from SH-SY5Y cells were obtained as described previously [24]. Proteins were electrophoresed by SDS/PAGE and blotted on to nitrocellulose membrane (Bio-Rad Laboratories). Monoclonal anti-SOD1 and anti-Hsp60 (heat-shock protein 60) antibodies (Santa Cruz Biotechnology) were used as loading/purity controls of cytosolic and mitochondrial fractions respectively. Monoclonal anti-p53 (clone BP5312) (Sigma), anti-actin (Sigma), anti-[phospho-AMPKα (Thr^{172})] (Cell Signaling Technology) and anti-GAPDH (glyceraldehyde-3-phosphate dehydrogenase) (Santa Cruz Biotechnology) antibodies or polyclonal anti-AMPK (Santa Cruz Biotechnology), anti-Bax (Santa Cruz Biotechnology), anti-p38^{MAPK} (Santa Cruz Biotechnology) and anti-[phospho-p38^{MAPK} (Thr^{180}/Tyr^{182})] (Invitrogen) antibodies were used as primary antibodies. The specific protein complex, formed upon specific secondary antibody treatment, was identified using a Fluorchem Imaging system (Alpha Innotech) after incubation with ChemiGlow chemoluminescence substrate (Alpha Innotech). Densitometric analyses were calculated using Quantity One software (Bio-Rad Laboratories).

Protein determination

Proteins concentrations were determined according to the method described by Lowry et al. [34].

Data presentation

All experiments were carried out at least five different times, unless otherwise indicated. The results are means ± S.D. Statistical evaluation was conducted by ANOVA, followed by correction with a Bonferroni's test. Comparisons were considered to be significant at $P < 0.05$.

RESULTS AND DISCUSSION

AMPK is upstream of p38^{MAPK} and p53 in the phosphorylation cascade culminating in [Cu(isaepy)$_2$]-induced apoptosis

A close dependence between AMPK and p38^{MAPK} in the phosphorylation cascade leading to energetic/oxidative-stress-dependent apoptosis is emerging [8,18], and a p38^{MAPK}-dependent phospho-activation of p53 can occur upon chemical and physical stresses [18,33,35]. Previously, we have demonstrated that [Cu(isaepy)$_2$]-mediated cell death in SH-SY5Y cells was associated with AMPK and p53 up-regulation [28,29]. Therefore we determined whether AMPK and p53 activation were events requiring the intermediate induction of p38^{MAPK}. To this aim, we analysed the expression and phosphorylation levels of these proteins upon treatment with 50 μM [Cu(isaepy)$_2$] (Figure 1A). Although the basal levels of AMPK and p38^{MAPK} remained unchanged during the treatment, phospho-AMPK and phospho-p38^{MAPK}, as well as p53, rapidly increased as soon as 1 h after [Cu(isaepy)$_2$] addition (Figure 1B). Moreover, further analyses indicated that these effects were dose-dependent in the micromolar range (see Supplementary Figure S1 at http://www.BiochemJ.org/bj/437/bj4370443add.htm). To verify whether p38^{MAPK} and p53 were AMPK-responsive factors, we took advantage of cells overexpressing the non-phosphorylatable D/N form (T172A) of the α2 subunit of AMPK (AMPK D/N cells), treated them with [Cu(isaepy)$_2$] and evaluated whether p53 and phospho-p38^{MAPK} were modulated in these conditions. Consistent with our previous results [29], cytofluorimetric analyses indicated that AMPK D/N cells were resistant to [Cu(isaepy)$_2$]-induced apoptosis (Figure 1B). Compared with normal cells, a lower, but still measurable, activation of both p38^{MAPK} and p53 was also observed under these conditions (Figure 1D). To confirm the tight dependence of p38^{MAPK} and p53 activation on AMPK phosphorylation, we evaluated the localization of phospho-p38^{MAPK} and p53 in AMPK D/N cells by fluorescence microscopy. Figure 1(E) shows that, in line

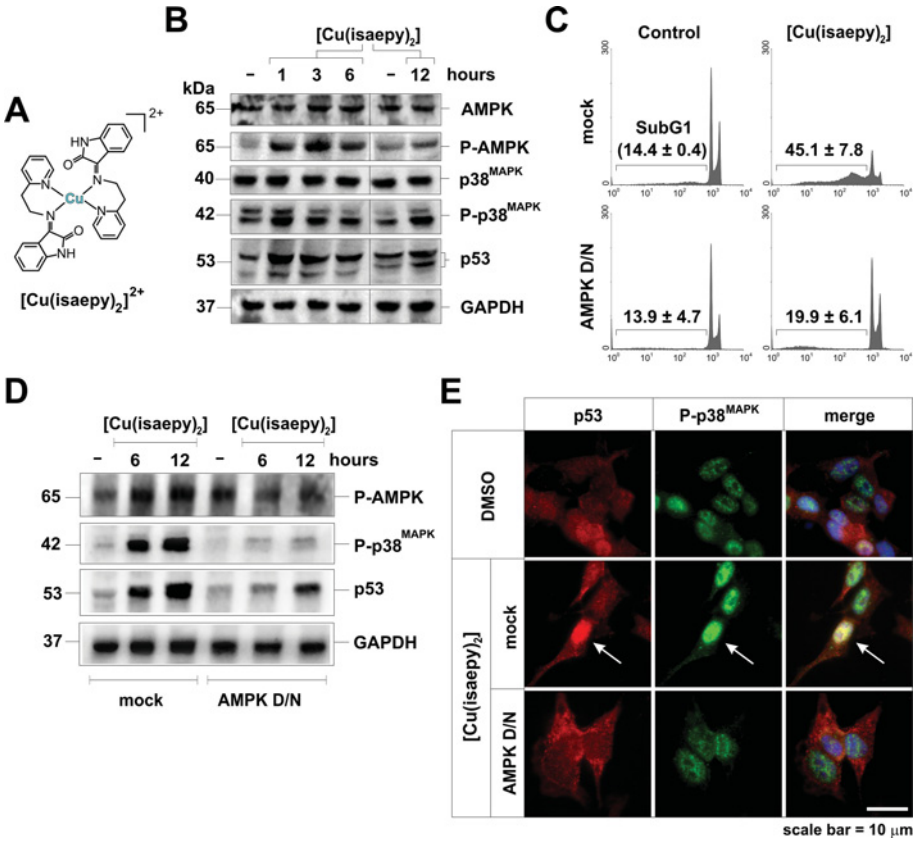

Figure 1 p38^{MAPK} and p53 are activated downstream of AMPK upon treatment with [Cu(isaepy)$_2$]

(**A**) Structure of [Cu(isaepy)$_2$]. (**B**) SH-SY5Y cells were treated with 50 μM [Cu(isaepy)$_2$] or, as a control, with equal volumes of DMSO. At the indicated times, 30 μg of total protein extract was loaded on to each lane for the detection of basal and phospho-activated levels of AMPK and p38^{MAPK}, as well as p53. GAPDH was used as a loading control. Western blots are from one experiment and are representative of three that gave similar results. Molecular-mass markers are shown on the left. (**C**) SH-SY5Y cells were transfected with the D/N (T172A) mutant of AMPK (AMPK D/N) or with an empty vector (mock). At 48 h after transfection, cells were treated with 50 μM [Cu(isaepy)$_2$] for 24 h or, as control, with equal volumes of DMSO, and washed and stained with propidium iodide. Analyses of the extent of apoptosis (SubG$_1$) were performed using a FACScalibur instrument, and percentages of staining-positive cells were calculated using WinMDI version 2.8 software. Cell-cycle plots are from a typical experiment performed in triplicate out of five that gave similar results. (**D**) Mock and AMPK D/N SH-SY5Y cells were treated with 50 μM [Cu(isaepy)$_2$] for 6 and 12 h or, as control, with equal volumes of DMSO. Total protein extract (30 μg) was loaded on to each lane for the immunodetection of phospho-AMPK, phospho-p38^{MAPK} and p53. GAPDH was used as loading control. Western blots are from one experiment and are representative of three that gave similar results. Molecular-mass markers are shown on the left. (**E**) Mock and AMPK D/N SH-SY5Y cells were treated for 6 h with 50 μM [Cu(isaepy)$_2$], washed, fixed in 4 % paraformaldehyde and permeabilized. Phospho-p38^{MAPK} and p53 were visualized upon staining with specific antibodies and probed further with Alexa Fluor® 488- and Alexa Fluor® 568-conjugated secondary antibodies respectively. To visualize nuclei, cells were also incubated with the cell-permeant DNA dye Hoechst 33342. Images shown are from one experiment and are representative of three that gave similar results. Untreated parental SH-SY5Y cells (DMSO) were used as controls.

with the results described above, the nuclear localization of both p38^{MAPK} and p53 was reduced in cells where AMPK phospho-activation was prevented. These results suggest that the activation of AMPK and p38^{MAPK} are connected to each other along a unique phosphorylation cascade governing cell responses to [Cu(isaepy)$_2$] and culminating in p53-dependent cell death.

p38^{MAPK} mediates [Cu(isaepy)$_2$] toxicity and regulates p53 activation

p53 gains transcriptional activity downstream of phosphorylation events mediated by different protein kinases, such as AMPK and p38^{MAPK} [8,9,18]. To establish whether p53 is an exclusive target of AMPK or p38^{MAPK}, we knocked down p38^{MAPK} using the siRNA technique and analysed both cell death and p53 expression levels upon 24 h of treatment with 50 μM [Cu(isaepy)$_2$]. Figure 2(A) shows cytofluorimetric analyses, upon staining with propidium iodide, of SH-SY5Y cells transfected with two alternative siRNAs against p38^{MAPK} (sip38$_1$ and sip38$_2$ cells) or with a scrambled 21-nucleotide RNA sequence (siScr cells). In particular, the results indicated that both sip38 cells had a smaller subG$_1$ (apoptotic) population than their siScr counterparts, with sip38$_1$ cells being more resistant to [Cu(isaepy)$_2$]-induced toxicity. In line with this finding, no increase in p53 immunoreactivity was observed in sip38$_1$ cells at each time point examined (Figure 2B), indicating that p53 activation depended only on p38^{MAPK}. Similar results were also obtained in cells overexpressing the KM of p38^{MAPK} (p38-KM cells), which is still activatable by upstream kinases, but is unable to phosphorylate downstream targets. Figure 2(C) shows that p38-KM cells were significantly rescued from [Cu(isaepy)$_2$]-induced apoptosis. Consistent with this observation, despite a sustained increase in the immunoreactivity of phospho-p38^{MAPK}, no significant increment in p53 expression levels was obtained (Figure 2D), suggesting that, upon treatment with [Cu(isaepy)$_2$], p38^{MAPK} is the molecular link between AMPK and p53.

The AMPK/p38^{MAPK}/p53 signalling axis is responsive to [Cu(isaepy)$_2$]-mediated energetic impairment

We have reported previously that [Cu(isaepy)$_2$] induces oxidative phosphorylation dysfunction, which finally leads to $\Delta\Psi_m$ (mitochondrial transmembrane potential) loss and a decrease in

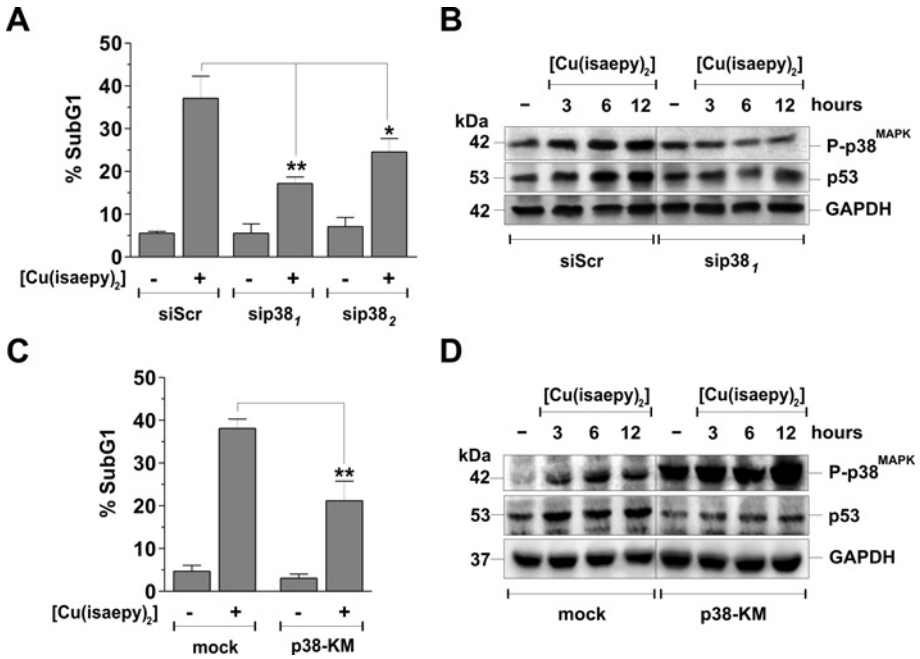

Figure 2 Inhibition of p38^{MAPK} activation results in a decrease in p53 accumulation and apoptosis induced by [Cu(isaepy)$_2$]

(**A**) SH-SY5Y cells were transfected with two siRNAs against p38^{MAPK} (sip38$_1$ or sip38$_2$) or with a scrambled siRNA sequence (siScr). After 12 h, cells were treated for a further 24 h with 50 μM [Cu(isaepy)$_2$] or, as a control, with equal volumes of DMSO, and stained with propidium iodide and analysed cytofluorimetrically for the extent of apoptosis. Results are expressed as a percentage of subG$_1$ (apoptotic) cells and are the means $\pm$ S.D. for four independent experiments. *$P < 0.05$ and **$P < 0.01$. (**B**) siScr and sip38$_1$ cells were treated with 50 μM [Cu(isaepy)$_2$] or, as control, with equal volumes of DMSO. At the indicated times, 30 μg of total protein extract was loaded on to each lane for the immunodetection of phospho-p38^{MAPK} and p53. GAPDH was used as a loading control. Western blots are from one experiment and are representative of three that gave similar results. Molecular-mass markers are shown on the left. (**C**) SH-SY5Y cells were transfected with a KM form of p38^{MAPK} (p38-KM) or with an empty vector (mock). At 48 h after transfection, mock and p38-KM cells were treated for 24 h with 50 μM [Cu(isaepy)$_2$] or, as control, with equal volumes of DMSO, and stained with propidium iodide and analysed cytofluorimetrically for the extent of apoptosis. Results are expressed as a percentage of SubG$_1$ (apoptotic) cells and are the means $\pm$ S.D. for four independent experiments. **$P < 0.01$. (**D**) Mock and p38-KM cells were treated with 50 μM [Cu(isaepy)$_2$] or, as a control, with equal volumes of DMSO. At the indicated times, 30 μg of total protein extract was loaded on to each lane for the immunodetection of phospho-p38^{MAPK} and p53. GAPDH was used as a loading control. Western blots are from one experiment and are representative of three that gave similar results. Molecular-mass markers are shown on the left.

ATP [29]. To assess whether activation of the AMPK/p38^{MAPK}/p53 signalling pathway relied upon [Cu(isaepy)$_2$]-mediated energetic impairment, we incubated the cells with fuel supplies that enter metabolic pathways at different points: 30 mM glucose, 10 mM pyruvate and 10 mM succinate, as the esterified form of methyl succinate. Then, the cells were treated with 50 μM [Cu(isaepy)$_2$] for 24 h and apoptosis was evaluated cytofluorimetrically. Figure 3(A) shows that, although to differing extents, these compounds decreased the percentage of apoptotic cells. It is also worth noting that the number of apoptotic cells measured upon incubation with glucose and succinate was significantly lower than those treated with pyruvate, confirming that ATP deriving from glycolysis or generated bypassing mitochondrial Complex I was sufficient, at least in part, to counteract [Cu(isaepy)$_2$]-mediated energetic stress and apoptosis. Therefore we performed Western blot analyses of phospho-p38^{MAPK} and p53 under the same conditions. Figure 3(B) shows that the addition of glucose and succinate decreased phospho-p38^{MAPK} and p53 immunoreactivity to an extent correlating with their capability to rescue cells from death. Conversely, pyruvate only weakly countered AMPK/p38^{MAPK}/p53 activation, in a way resembling the weak protection exerted against [Cu(isaepy)$_2$]-induced apoptosis.

It has been demonstrated recently that RA enhances metabolic-stress-stimulated glucose uptake in skeletal muscle cells [37]. As we found previously that incubation with RA completely rescued cells from [Cu(isaepy)$_2$]-induced apoptosis [28], we wondered whether this event was mediated by an increase in glucose uptake and a consequent modulation of the AMPK-dependent signalling axis. Therefore we analysed whether RA influenced glucose uptake in SH-SY5Y cells by evaluating cytofluorimetrically the incorporation of 2-NBDG, a fluorescent analogue of the non-phosphorylatable 2-deoxy-D-glucose. Figure 3(C) shows that, incubation with RA significantly increased 2-NBDG uptake, confirming that this process is also active in SH-SY5Y cells. Next, the cells were incubated with 20 μM RA, treated with 50 μM [Cu(isaepy)$_2$] and activation of the AMPK/p38^{MAPK}/p53 pathway was analysed by Western blotting. Figure 3(D) shows that RA incubation prevented the accumulation of phospho-AMPK and phospho-p38^{MAPK}, as well as of p53. Results obtained in these experiments were consistent with the hypothesis that [Cu(isaepy)$_2$] induced metabolic stress, and confirmed that either cell re-feeding with different fuel supplies or an increase in glucose uptake reduced [Cu(isaepy)$_2$]-induced cytotoxicity by weakening the activation of the AMPK/p38^{MAPK}/p53 signalling pathway.

AMPK/p38^{MAPK}/p53 axis is not a prototype of DLC-responsive signalling pathways

As we have characterized [Cu(isaepy)$_2$] as a molecule belonging to the DLC class, we wondered whether the activation of the AMPK/p38^{MAPK}/p53 axis was specific for [Cu(isaepy)$_2$] or a general cell response towards other DLCs differently affecting mitochondrial function. To this aim, we selected DQC and Rho123, the former specifically targeting Complex I and the latter affecting F_1F_0-ATPase activity. After dose–response experiments (results not shown), we chose a concentration of 100 μM for both compounds because it showed an extent of apoptosis similar to

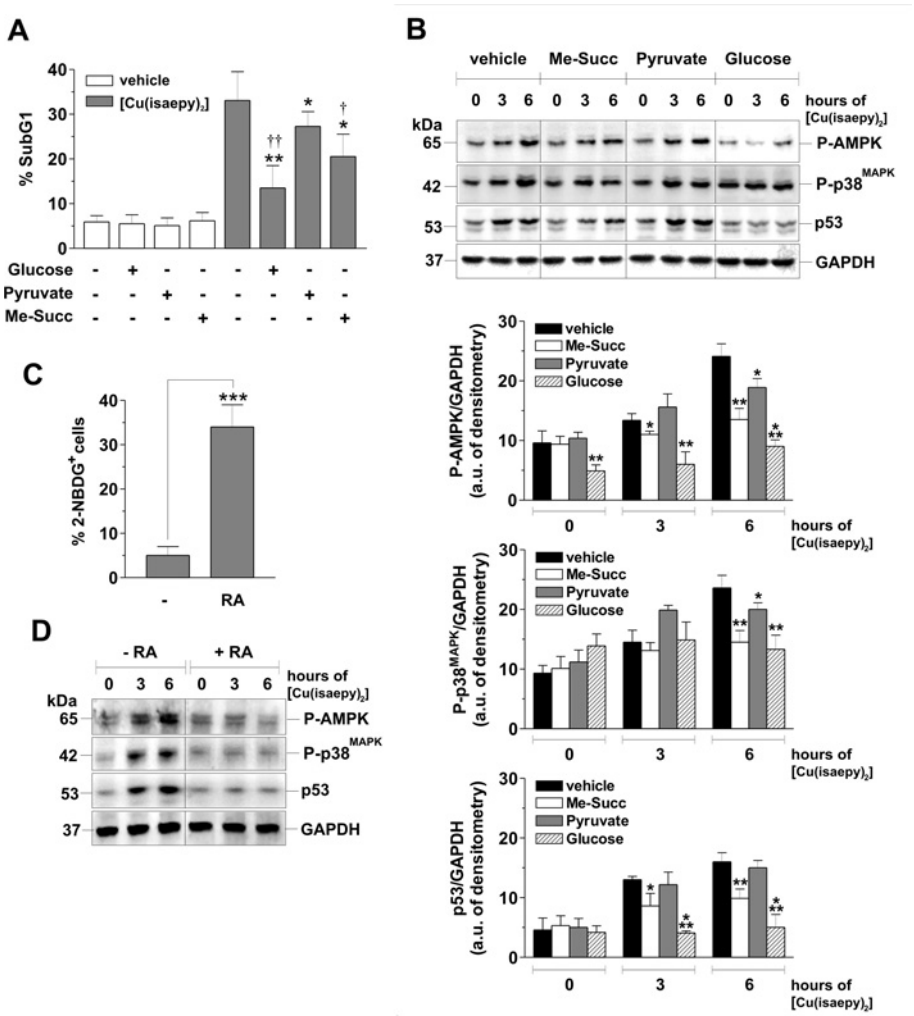

Figure 3 Increased availability of fuel supplies inversely correlates with the activation of the AMPK/p38^{MAPK}/p53 signalling axis and apoptosis induced by [Cu(isaepy)$_2$]

(**A**) SH-SY5Y cells were treated for 24 h with 50 μM [Cu(isaepy)$_2$] or, as control, with equal volumes of DMSO, in medium supplemented with 30 mM glucose, 10 mM pyruvate or 10 mM methyl succinate (Me-Succ), stained with propidium iodide and analysed cytofluorimetrically for the extent of apoptosis. As a control for administration of fuel supplies, equal volumes of PBS were added to the cell culture medium. Results are expressed as a percentage of subG$_1$ (apoptotic) cells and are the means $\pm$ S.D. for four independent experiments. $^*P < 0.05$; $^{**}P < 0.01$ compared with [Cu(isaepy)$_2$]-treated cells; †$P < 0.05$ and ††$P < 0.01$ compared with [Cu(isaepy)$_2$]-treated cells incubated with pyruvate. (**B**) Alternatively, at the indicated times, 30 μg of total protein extract was loaded on to each lane for the immunodetection of the phospho-activated levels of AMPK and p38^{MAPK}, as well as p53. GAPDH was used as a loading control. Western blots are from one experiment and are representative of three that gave similar results. Densitometric analyses of phospho-AMPK, phospho-p38^{MAPK}, p53 and GAPDH were calculated using Quantity One software. Results are expressed as phospho-AMPK/GAPDH, phospho-p38^{MAPK}/GAPDH and p53/GAPDH ratios, and are means $\pm$ S.D. $^*P < 0.05$, $^{**}P < 0.01$ and $^{***}P < 0.001$. Molecular-mass markers are shown on the left. (**C**) SH-SY5Y cells were grown for 2 weeks in the presence 20 μM RA or, as a control, with equal volumes of DMSO. Afterwards, they were incubated with 100 μM 2-NBDG for 1 h, washed to stop 2-NBDG uptake and collected, and fluorescence was analysed cytofluorimetrically using WinMDI 2.8 software. Results are expressed as a percentage of 2-NBDG-positive cells and are means $\pm$ S.D. of three independent experiments. $^{***}P < 0.001$. (**D**) RA-differentiated cells were treated with 50 μM [Cu(isaepy)$_2$] or, as a control, with equal volumes of DMSO. At the indicated times, 30 μg of total protein extract was loaded on to each lane for the immunodetection of the phospho-activated levels of AMPK and p38^{MAPK}, as well as p53. GAPDH was used as a loading control. Western blots are from one experiment and are representative of three that gave similar results. Molecular-mass markers are shown on the left.

those achieved with [Cu(isaepy)$_2$]. Indeed, after 24 h of treatment with both DQC and Rho123, approximately 30 % of SH-SY5Y cells underwent cell death (Figure 4A). This phenomenon correlated well with an increase in the immunoreactivity of p53 (Figure 4B) after 6 and 12 h of treatment, suggesting that p53 could be associated with cell death mechanisms downstream of mitochondrial dysfunction. However, no phospho-activation of AMPK and p38^{MAPK} was observed (Figure 4B), indicating that this signalling axis was specific for [Cu(isaepy)$_2$]. To validate these assumptions, we incubated the cells with 20 μM pifithrin-α, a chemical inhibitor of p53 or, alternatively, overexpressed the inactive AMPK D/N, and then analysed the extent of apoptosis after 24 h of treatment with 100 μM Rho123 and DQC. As shown in Figure 4(C), no protection against Rho123- and DQC-induced toxicity was achieved in either of the experimental conditions, indicating that the AMPK/p38^{MAPK}/p53 signalling pathway is exclusive for [Cu(isaepy)$_2$], whereas different mechanisms are involved in the induction of cell death downstream of conventional DLCs.

3BrPA enhances [Cu(isaepy)$_2$] cytotoxicity by enhancing metabolic oxidative stress

One of the main purposes of cancer therapy is to be less aggressive towards normal tissues, but efficient enough to kill transformed cells and to avoid cell resistance. To reach this goal, a combined

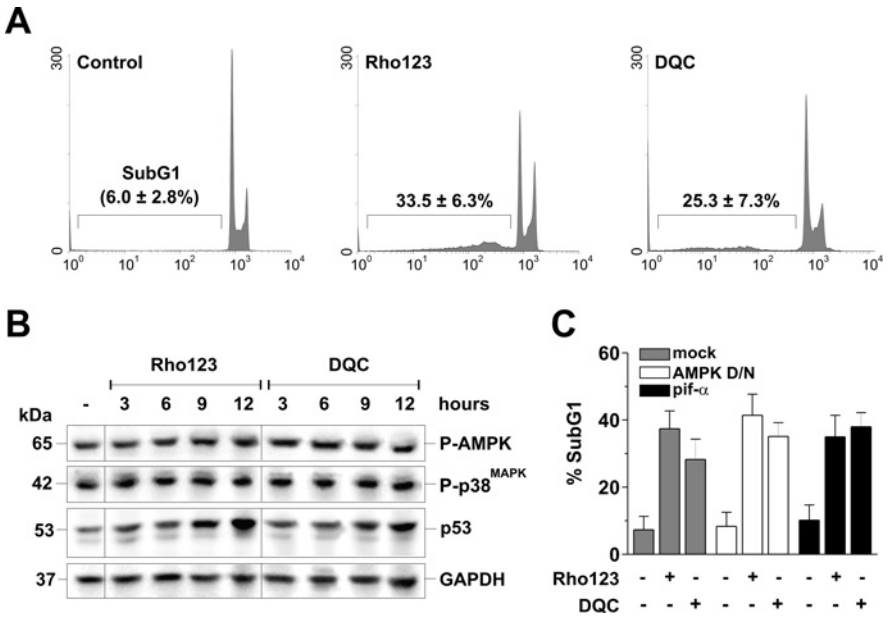

Figure 4 The DLCs DQC and Rho123 induce apoptosis independently of the activation of the AMPK/p38^{MAPK}/p53 signalling axis

(**A**) SH-SY5Y cells were treated for 24 h with 100 μM DQC), Rho123 or, as control, with equal volumes of PBS or DMSO, and subsequently washed and stained with propidium iodide. Analyses of the extent of apoptosis (subG$_1$) were calculated using WinMDI version 2.8 software. The cell-cycle plots shown are from a typical experiment performed in triplicate out of five that gave similar results. (**B**) Alternatively, at the indicated times, 30 μg of total protein extract was loaded on to each lane for the immunodetection of the phospho-activated levels of AMPK and p38^{MAPK}, as well as p53. GAPDH was used as a loading control. Western blots are from one experiment and are representative of three that gave similar results. Molecular-mass markers are shown on the left. (**C**) Mock, AMPK D/N and parental SH-SY5Y cells incubated with 10 μM of the pharmacological inhibitor of p53, pifithrin-α (pif-α) or, as a control, equal volumes of DMSO, were treated for 24 h with 100 μM DQC or Rho123, stained with propidium iodide and analysed cytofluorimetrically for the extent of apoptosis. Results are expressed as a percentage of subG$_1$ (apoptotic) cells and are means ± S.D. for four independent experiments.

therapy is often used. Therefore we attempted to decrease the concentration of [Cu(isaepy)$_2$] to doses that do not induce apoptosis and employed it in combination with the glycolytic inhibitor 3BrPA, which eradicates liver cancer in animals without associated systemic toxicity [38]. 3BrPA was discovered as an efficient inhibitor of hexokinase II [39,40], and only recently characterized to also affect succinate dehydrogenase activity [41], thus providing the molecular bases of its antitumour property. Figure 5(A) shows that SH-SY5Y cells underwent apoptosis when 10 μM [Cu(isaepy)$_2$] and 10 μM 3BrPA were used in combination, whereas no toxicity was observed when the same concentrations of [Cu(isaepy)$_2$] and 3BrPA were administered separately. To assess whether the AMPK/p38^{MAPK}/p53 signalling axis was also activated under these conditions, we performed Western blot analyses of the expression levels of these proteins. Figure 5(B) shows that the phosphorylated form of AMPK and p38^{MAPK}, and the protein levels of p53 significantly increased only upon the combined treatment, whereas they remained unchanged when [Cu(isaepy)$_2$] and 3BrPA were used alone.

Taken together, these preliminary results indicated that the addition of 3BrPA, a further energy-depleting molecule, allowed a decrease in the concentrations of [Cu(isaepy)$_2$] used to achieve the same toxic effects in neuroblastoma cells. We then used PCNs to evaluate the toxic effects of [Cu(isaepy)$_2$]. In particular, incubation with 50 μM [Cu(isaepy)$_2$] for 24 h yielded widespread cell death with features of necrosis (results not shown), indicating that [Cu(isaepy)$_2$] was toxic even in untransformed cells when used at high doses. This observation prompted us to perform combined treatments with low doses of both [Cu(isaepy)$_2$] and 3BrPA in order to minimize their side effects in healthy cells. To verify whether these conditions were tolerated by PCNs, we treated the cells with 10 μM [Cu(isaepy)$_2$] and/or 10 μM 3BrPA for 24 h and analysed the induction of apoptosis by counting condensed/fragmented nuclei upon Hoechst 33342 staining and by evaluating caspase 3 cleavage by fluorescence microscopy. Figures 5(C) and 5(D) show that, in comparison with the results observed in SH-SY5Y cells, neither single nor combined treatment with [Cu(isaepy)$_2$] and 3BrPA, at low doses, induced a significant activation of apoptosis. To assess whether this different sensitivity was associated with the different glycolytic metabolism between SH-SY5Y cells and PCNs, we next analysed the extracellular lactate concentration, which is a suitable marker of glycolysis. Figure 5(E) indicates that PCNs had a much lower glycolytic rate than their neuroblastoma counterparts, which was corroborated by 10-fold less basal levels of lactate in the extracellular space. Moreover, in PCNs, lactate production was not affected by treatment with [Cu(isaepy)$_2$] or 3BrPA, whereas it was significantly decreased when SH-SY5Y cells were treated with 3BrPA, indicating that, by inhibiting the tumour-specific isoform hexokinase II, 3BrPA mainly affects glycolytic metabolism of neuroblastoma cells, but was virtually ineffective in PCNs. This result indicated that a metabolic stress could be implicated in the apoptotic response of neuroblastoma cells to the combined treatment of [Cu(isaepy)$_2$] and 3BrPA, although it mainly depended on the contribution of 3BrPA.

To assess the role of oxidative stress in the toxicity of the combined treatment, we evaluated relative ROS production upon incubation with DCFH-DA. Figure 6(A) shows that [Cu(isaepy)$_2$] and 3BrPA yielded an increase in intracellular ROS in SH-SY5Y cells when employed alone or in combination, whereas only a very small, although significant, effect was observed in PCNs. To investigate this issue further, we took advantage of an SH-SY5Y cell line overexpressing the WT form of the human antioxidant enzyme SOD1 (*h*SOD cells) [28]. Both parental and SOD1-overexpressing SH-SY5Y cells were treated with 10 μM [Cu(isaepy)$_2$] in the presence of 10 μM 3BrPA for 24 h, and

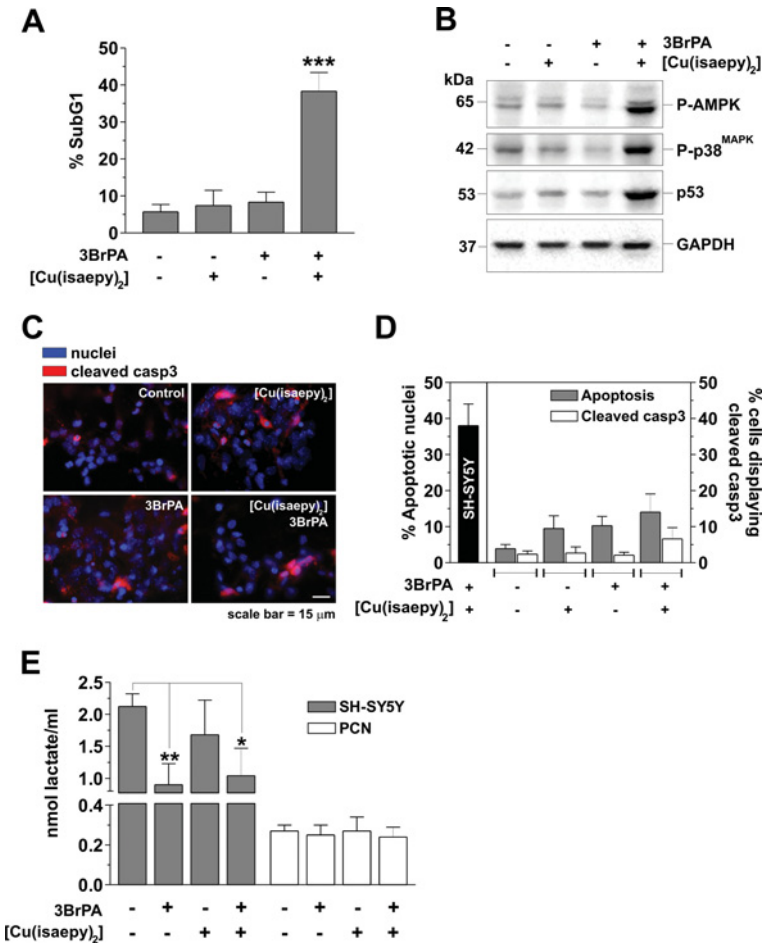

Figure 5 3BrPA enhances the activation of the AMPK/p38^{MAPK}/p53 signalling axis and apoptosis induced by [Cu(isaepy)$_2$]

(**A**) SH-SY5Y cells were treated with 10 μM [Cu(isaepy)$_2$] or, as control, with equal volumes of DMSO in the presence or absence of 10 μM 3BrPA, dissolved in PBS, for 24 h, stained with propidium iodide and analysed cytofluorimetrically for the extent of apoptosis. Results are expressed as a percentage of subG$_1$ (apoptotic) cells and are means $\pm$ S.D. for four independent experiments. ***$P < 0.001$. (**B**) Alternatively, after 6 h of treatment, 30 μg of total protein extract was loaded on to each lane for the immunodetection of the phospho-activated levels of AMPK and p38^{MAPK}, as well as p53. GAPDH was used as a loading control. Western blots are from one experiment and are representative of three that gave similar results. Molecular-mass markers are shown on the left. (**C**) PCNs were treated with 10 μM [Cu(isaepy)$_2$] or, as a control, with equal volumes of DMSO in the presence or absence of 10 μM 3BrPA for 24 h, washed, fixed in 4 % paraformaldehyde and permeabilized. Cleaved caspase 3 was visualized upon staining with a specific antibody and probed further with an Alexa Fluor® 568-conjugated secondary antibody. To visualize nuclei, cells were also incubated with the cell-permeant DNA dye Hoechst 33342. The images shown are from one experiment out of five that gave similar results, the percentages of which are shown in (**D**), along with the extent of apoptosis in SH-SY5Y cells measured upon the combined treatment (black bar). Results are expressed as a percentage of cells displaying apoptotic nuclei or cleaved caspase 3 and are means $\pm$ S.D. for four independent experiments. (**E**) SH-SY5Y cells and PCNs were treated with 10 μM [Cu(isaepy)$_2$] or, as a control, with equal volumes of DMSO in the presence or absence of 10 μM 3BrPA for 6 h. Cell medium was then collected and lactate was determined spectrophotometrically following the reduction of NAD$^+$ at 340 nm. Results are expressed as nmol of lactate/ml and are means $\pm$ S.D. for three independent experiments. *$P < 0.05$ and **$P < 0.01$.

apoptosis was then analysed cytofluorimetrically. Figure 6(B) shows that, under these conditions, the percentage of apoptosis was reduced by 50 % in *h*SOD cells, and the levels of phospho-AMPK, phospho-p38^{MAPK}and p53 were reduced (Figure 6C). This result clearly indicated that the different susceptibility of the cells correlated with a different degree of activation of the AMPK/p38^{MAPK}/p53 signalling axis, and concomitantly suggested that, besides energetic impairment, oxidative stress taking place downstream of [Cu(isaepy)$_2$]/3BrPA co-treatment resulted in the selective toxicity of these molecules in neuroblastoma cells.

To explain the different susceptibility between SH-SY5Y cells and PCNs to the [Cu(isaepy)$_2$]/3BrPA combined treatment, we measured the activity of the antioxidant enzymes SOD1, glutathione peroxidase and catalase in both cell types; however, no significant difference was observed (results not shown). Measurements of extracellular lactate (Figure 5E) and several lines of evidence from the literature [42] indicate that PCNs, such as many other non-proliferating cell types, redirect the majority of glucose, taken up from the extracellular space, towards the oxidative branch of the pentose phosphate pathway to generate NADPH, rather than utilize it as glycolytic substrate. This metabolic strategy should ensure a more 'reducing' intracellular milieu, which responds better to oxidative challenges. We then hypothesized that the shift in the glycolytic compared with the pentose phosphate pathway, and in turn the levels of NADPH, could represent the determinant of the different sensitivity to [Cu(isaepy)$_2$]/3BrPA co-treatment observed in neuroblastoma cells and PCNs. To verify this issue, PCNs were grown in a low-glucose-containing milieu or, alternatively, in the presence of 1 μM DHEA, a glucose-6-phosphate dehydrogenase inhibitor, and then the cells were subjected to the combined treatment. Figure 6(D) shows that, under both of these conditions, PCNs became susceptible to [Cu(isaepy)$_2$]/3BrPA treatment, with high percentages of cells displaying apoptotic nuclei. To assess whether oxidative stress took place under these conditions, we evaluated, by Western blot analyses, the protein carbonyl content, one

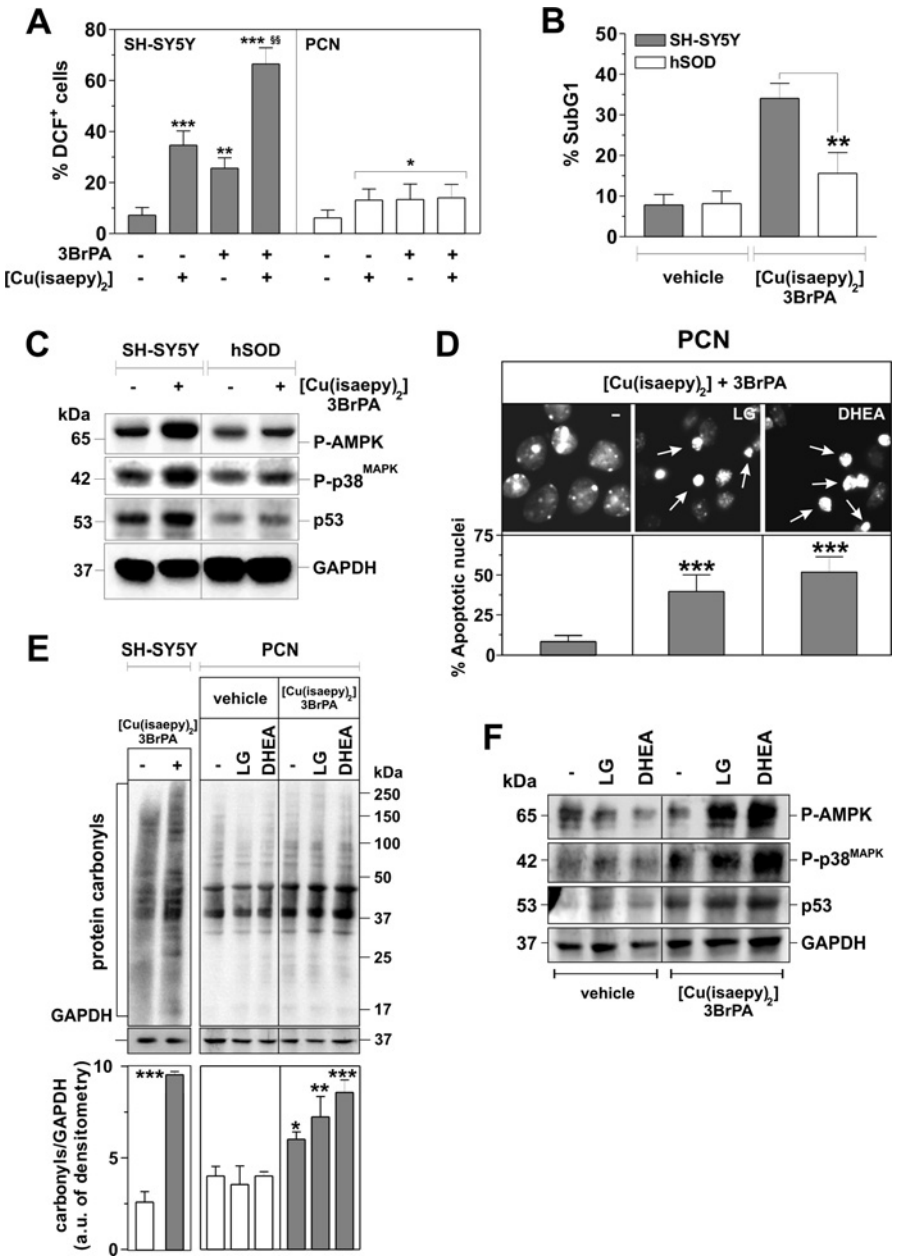

Figure 6 Oxidative conditions contribute to the AMPK/p38^{MAPK}/p53 signalling axis and apoptosis induced by the combination of [Cu(isaepy)$_2$] and 3BrPA

(**A**) SH-SY5Y cells and PCNs were treated with 10 μM [Cu(isaepy)$_2$] or, as a control, with equal volumes of DMSO in the presence or absence of 10 μM 3BrPA (dissolved in PBS) for 6 h and incubated with 50 μM DCFH-DA. Cells were then washed with PBS and ROS production was analysed cytofluorimetrically. Results are expressed as a percentage of DCF$^+$ cells and are means $\pm$ S.D. for four independent experiments. $^*P < 0.05$, $^{**}P < 0.01$ and $^{***}P < 0.001$ compared with control; §§ $P < 0.01$ compared with [Cu(isaepy$_2$)-treated cells. (**B**) Parental or SOD1-overexpressing (hSOD) SH-SY5Y cells were treated with 10 μM [Cu(isaepy)$_2$] or, as a control, with equal volumes of DMSO in the presence of 10 μM 3BrPA for 24 h, stained with propidium iodide and analysed cytofluorimetrically for the extent of apoptosis. Results are expressed as a percentage of subG$_1$ (apoptotic) cells and are means $\pm$ S.D. for four independent experiments. $^{**}P < 0.01$. (**C**) Alternatively, after 6 h of treatment, 30 μg of total protein extract was loaded on to each lane for the immunodetection of the phospho-activated levels of AMPK and p38^{MAPK}, as well as p53. GAPDH was used as a loading control. Western blots are from one experiment and are representative of three that gave similar results. Molecular-mass markers are shown on the left. (**D**) PCNs were grown in medium containing 5 mM glucose [low glucose (LG)] or in the presence of 1 μM DHEA, a glucose-6-phosphate dehydrogenase inhibitor or, as a control, with equal volumes of DMSO. PCNs were then subjected to the combined treatment with 10 μM [Cu(isaepy)$_2$] and 3BrPA for 24 h, washed, fixed in 4 % paraformaldehyde and permeabilized. Apoptotic nuclei were visualized upon staining with the cell-permeant DNA dye Hoechst 33342. Images shown are from one experiment out of five that gave similar results, the percentages of which are shown in the lower panel. Results are expressed as a percentage of cells displaying apoptotic nuclei and are means $\pm$ S.D. for four independent experiments. $^{***}P < 0.001$. (**E**) PCNs were grown in low-glucose-containing medium, in the presence of 1 μM DHEA or, as a control, with equal volumes of DMSO and then subjected to the combined treatment with 10 μM [Cu(isaepy)$_2$] and 3BrPA. Total protein extract (30 μg) was loaded on to each lane for the immunodetection of protein carbonyls. Carbonyls from SH-SY5Y cells treated with the combined treatment are also shown. GAPDH was used as a loading control. Densitometric analyses were performed using Quantity One software. Results are expressed as the carbonyl/GAPDH ratio and are means $\pm$ S.D. $^*P < 0.05$, $^{**}P < 0.01$ and $^{***}P < 0.001$. (**F**) PCNs were grown in low-glucose-containing medium, in the presence of 1 μM DHEA or, as a control, with equal volumes of DMSO and then subjected to the combined treatment with 10 μM [Cu(isaepy)$_2$] and 3BrPA. Total protein extract (30 μg) was loaded on to each lane for the immunodetection of the phospho-activated levels of AMPK and p38^{MAPK}, as well as p53. GAPDH was used as a loading control. Western blots are from one experiment and are representative of three that gave similar results. Molecular-mass markers are shown on the left.

of the principal markers of occurring oxidative damage. SH-SY5Y cells showed a significant increase in protein carbonylation upon [Cu(isaepy)$_2$]/3BrPA treatment (Figure 6E), confirming the high production of ROS measured previously (Figure 6A). Conversely, PCNs did not display any relevant change in protein carbonyls, unless they were grown in low-glucose medium or incubated with DHEA (Figure 6E), conditions for which Western blot analyses showed an increase in phospho-AMPK, phospho-p38^{MAPK} and p53 immunoreactivity (Figure 6F). Overall these results suggest that, even in PCNs, cell death phenomena and oxidative damage downstream of [Cu(isaepy)$_2$]/3BrPA co-treatment were reasonably associated with the activation of the AMPK/p38^{MAPK}/p53 signalling axis.

Conclusions

We have demonstrated previously that [Cu(isaepy)$_2$] is a DLC-like molecule able to affect mitochondrial oxygen consumption and produce ROS, thereby resulting in p53-mediated and AMPK-dependent apoptosis [28,29]. On the basis of these results, in the present study, we have determined that apoptosis proceeds via the intermediate action of p38^{MAPK}, thereby delineating an AMPK/p38^{MAPK}/p53 signalling axis as the principal route controlling [Cu(isaepy)$_2$]-induced apoptosis, with AMPK being the upstream sensor, p38^{MAPK} the mediator and p53 the final executioner of the cell death programme. The inactivation of these proteins results in a significant reduction in the extent of apoptosis, although this value decreased in response to the protein targeted, with the inhibition of AMPK, p38^{MAPK} or p53 resulting in an 81, 52 or 32 % decrease in cell death respectively. These observations clearly suggest that other additional targets of either AMPK or p38^{MAPK} could exist and reasonably account for the remaining extent to reach the full recovery of cell viability.

In the search for the upstream event triggering the AMPK/p38^{MAPK}/p53 apoptotic axis, we have demonstrated that energy deficiency is profoundly implicated in [Cu(isaepy)$_2$]-mediated toxicity. The present results correlated well with the indication that the protective effects of RA towards [Cu(isaepy)$_2$] cytotoxicity depended on its ability to enhance glucose uptake [37]. This is in accordance with a glucose addiction typical of tumour cells, which allows the occurrence of anabolic reactions and the acidification of the stromal environment by increasing lactate release. In regard to these metabolic changes, ATP-depleting drugs (e.g. glycolytic inhibitors) have been recently exploited in cancer therapy. However, their use in single treatment did not gain the expected success, whereas their employment in combination with conventional chemotherapeutics affecting cellular homoeostasis (e.g. redox or metabolic stressors) seems to be more achievable [43], Results obtained in the present study have indicated that a combined treatment with low doses of [Cu(isaepy)$_2$] and 3BrPA, a potent glycolytic inhibitor, was effective and selective, as it induced apoptosis in neuroblastoma cells without any significant toxicity towards differentiated PCNs. 3BrPA can react with hexokinase II and succinate dehydrogenase [38–41], as well as the SH and hydroxy groups of other metabolic enzymes, such as pyruvate kinase [44], glutamate dehydrogenase [45], GAPDH [41,46,47] and 3-phosphoglycerate kinase [41], thereby inhibiting their activity by means of the formation of an irreversible covalent bond with its pyruvyl moiety. In particular, as hexokinase II is the specific mitochondria-located form of this enzyme in cancer cells, whose activity is pivotal for sustaining the high glycolytic rate of tumours (Warburg effect), the results obtained in the present study emphasize the pivotal role of hexokinase II in tumour glycolysis.

Findings from the literature report that 3BrPA is also a ROS producer [48,49]. Indeed, as 3BrPA inhibits hexokinase-mediated glucose phosphorylation, it is reasonable that not only cellular energetics, but also NADPH production via the pentose phosphate pathway could be hindered by treatment with 3BrPA. This assumption is consistent with the results obtained in SH-SY5Y cells, as well as in PCNs, in which the pentose phosphate pathway was affected. Nevertheless, the observations that other DLCs affecting ATP production and cell viability (e.g. Rho123 and DQC) did not activate the AMPK/p38^{MAPK}/p53 signalling pathway suggest that the unavailability of energetic equivalents does not represent the sole determinant of the antitumour effects of [Cu(isaepy)$_2$]. Indeed, fuel substrate administration, as well as the increase in SOD activity in *h*SOD cells, only partially inhibited activation of the AMPK/p38^{MAPK}/p53 axis and rescued cell viability in SH-SY5Y cells. Taken together, these results suggest that energy deficiency is certainly involved in [Cu(isaepy)$_2$]-mediated cell death, but pro-oxidant conditions generated upon [Cu(isaepy)$_2$] treatment, and enhanced by 3BrPA administration, are strongly expected to control the strength of the downstream apoptotic response.

AUTHOR CONTRIBUTION

Giuseppe Filomeni designed the research, analysed the experiments and wrote the paper. Simone Cardaci performed and analysed the experiments. Ana Maria Da Costa Ferreira synthesized [Cu(isaepy)$_2$]. Giuseppe Rotilio designed the research. Maria Ciriolo supervised the work, designed the research and wrote the paper. All authors discussed the manuscript prior to submission.

ACKNOWLEDGEMENT

We gratefully acknowledge Palma Mattioli for her technical assistance in fluorescence microscopy and image analyses.

FUNDING

This work was supported, in part, from the Ministero della Salute; Ministero dell'Istruzione, dell'Università e della Ricerca (MIUR), Associazione Italiana per la Ricerca sul Cancro (AIRC) [grant nunmber IG10636], the Brazilian agencies Fundação de Amparo a Pesquisa do Estado de São Paulo (FAPESP) [grant number 05/60596-8], Conselho Nacional de Desenvolvimento Científico e Tecnológico (CNPq, INCT Processos Redox em Biomedicina-Redoxoma), and Programma Esecutivo di Cooperazione Scientifica e Tecnologica Italia-Brasile [grant number #490021/2008-5].

REFERENCES

1 Hardie, D. G. (2007) AMP-activated/SNF1 protein kinases: conserved guardians of cellular energy. Nat. Rev. Mol. Cell Biol. **8**, 774–785
2 Hardie, D. G. and Sakamoto, K. (2006) AMPK: a key sensor of fuel and energy status in skeletal muscle. Physiology **21**, 48–60
3 Hue, L., Beauloye, C., Bertrand, L., Horman, S., Krause, U., Marsin, A. S., Meisse, D., Vertommen, D. and Rider, M. H. (2003) New targets of AMP-activated protein kinase. Biochem. Soc. Trans. **31**, 213–215
4 Inoki, K., Zhu, T. and Guan, K. L. (2003) TSC2 mediates cellular energy response to control cell growth and survival. Cell **115**, 577–590
5 Liang, J., Shao, S. H., Xu, Z. X., Hennessy, B., Ding, Z., Larrea, M., Kondo, S., Dumont, D. J., Gutterman, J. U., Walker, C. L. et al. (2007) The energy sensing LKB1-AMPK pathway regulates p27^{kip1} phosphorylation mediating the decision to enter autophagy or apoptosis. Nat. Cell Biol. **9**, 218–224
6 Ben Sahra, I., Laurent, K., Loubat, A., Giorgetti-Peraldi, S., Colosetti, P., Auberger, P., Tanti, J. F., Le Marchand-Brustel, Y. and Bost, F. (2008) The antidiabetic drug metformin exerts an antitumoural effect *in vitro* and *in vivo* through a decrease of cyclin D1 level. Oncogene **27**, 3576–3586
7 Sarbassov, D. D., Ali, S. M. and Sabatini, D. M. (2005) Growing roles for the mTOR pathway. Curr. Opin. Cell Biol. **17**, 596–603

8 Cao, C., Lu, S., Kivlin, R., Wallin, B., Card, E., Bagdasarian, A., Tamakloe, T., Chu, W. M., Guan, K. L. and Wan, Y. (2008) AMP-activated protein kinase contributes to UV- and H_2O_2 induced apoptosis in human skin keratinocytes. J. Biol. Chem. **283**, 28897–28908

9 Okoshi, R., Ozaki, T., Yamamoto, H., Ando, K., Koida, N., Ono, S., Koda, T., Kamijo, T., Nakagawara, A. and Kizaki, H. (2008) Activation of AMP-activated protein kinase induces p53-dependent apoptotic cell death in response to energetic stress. J. Biol. Chem. **283**, 3979–3987

10 Jones, RG, Plas, DR, Kubek, S, Buzzai, M, Mu, J, Xu, Y, Birnbaum, M. J. and Thompson, C. B. (2009) AMP-activated protein kinase induces a p53-dependent metabolic checkpoint. Mol. Cell **18**, 283–293

11 Rattan, R., Giri, S., Singh, A. K. and Singh, I. (2005) 5-Aminoimidazole-4-carboxamide-1-β-D-ribofuranoside inhibits cancer cell proliferation *in vitro* and *in vivo* via AMP-activated protein kinase. J. Biol. Chem. **280**, 39582–39593

12 Meisse, D., Van de Casteele, M., Beauloye, C., Hainault, I., Kefas, B. A., Rider, M. H., Foufelle, F. and Hue, L. (2002) Sustained activation of AMP-activated protein kinase induces c-Jun N-terminal kinase activation and apoptosis in liver cells. FEBS Lett. **526**, 38–42

13 Kefas, B. A., Cai, Y., Ling, Z., Heimberg, H., Hue, L., Pipeleers, D. and Van de Casteele, M. (2003) AMP-activated protein kinase can induce apoptosis of insulin-producing MIN6 cells through stimulation of c-Jun-N-terminal kinase. J. Mol. Endocrinol. **30**, 151–161

14 Fruman, D. A. and Edinger, A. L. (2008) Cancer therapy: staying current with AMPK. Biochem. J. **412**, e3–e5

15 Huang, X., Wullschleger, S., Shpiro, N., McGuire, V. A., Sakamoto, K., Woods, Y. L., McBurnie, W., Fleming, S. and Alessi, D. R. (2008) Important role of the LKB1–AMPK pathway in suppressing tumourigenesis in PTEN-deficient mice. Biochem. J. **412**, 211–221

16 Hwang, J. T., Kim, Y. M., Surh, Y. J., Baik, H. W., Lee, S. K., Ha, J. and Park, O. J. (2006) Selenium regulates cyclooxygenase-2 and extracellular signal-regulated kinase signalling pathways by activating AMP-activated protein kinase in colon cancer cells. Cancer Res. **66**, 10057–10063

17 Memmott, R. M., Gills, J. J., Hollingshead, M., Powers, M. C., Chen, Z., Kemp, B., Kozikowski, A. and Dennis, P. A. (2008) Phosphatidylinositol ether lipid analogues induce AMP-activated protein kinase-dependent death in LKB1-mutant non small cell lung cancer cells. Cancer Res. **68**, 580–588

18 Pan, W., Yang, H., Cao, C., Song, X., Wallin, B., Kivlin, R., Lu, S., Hu, G., Di, W. and Wan, Y. (2008) AMPK mediates curcumin-induced cell death in CaOV3 ovarian cancer cells. Oncol. Rep. **20**, 1553–1559

19 Kroemer, G. and Pouyssegur, J. (2008) Tumor cell metabolism: cancer's Achilles' heel. Cancer Cell **13**, 472–482

20 Vander Heiden, M. G., Cantley, L. C. and Thompson, C. B. (2009) Understanding the Warburg effect: the metabolic requirements of cell proliferation. Science **324**, 1029–1033

21 Dwarakanath, B. S. (2009) Cytotoxicity, radiosensitization, and chemosensitization of tumour cells by 2-deoxy-D-glucose *in vitro*. J. Cancer Res. Ther. **5**, S27–S31

22 Mathupala, S. P., Ko, Y. H. and Pedersen, P. L. (2009) Hexokinase-2 bound to mitochondria: cancer's stygian link to the "Warburg Effect" and a pivotal target for effective therapy. Semin. Cancer Biol. **19**, 17–24

23 Modica-Napolitano, J. S. and Aprille, J. R. (2001) Delocalized lipophilic cations selectively target the mitochondria of carcinoma cells. Adv. Drug Delivery Rev. **49**, 63–70

24 Simons, A. L., Ahmad, I. M., Mattson, D. M., Dornfeld, K. J. and Spitz, D. R. (2007) 2-Deoxy-D-glucose combined with cisplatin enhances cytotoxicity via metabolic oxidative stress in human head and neck cancer cells. Cancer Res. **67**, 3364–3370

25 Maschek, G., Savaraj, N., Priebe, W., Braunschweiger, P., Hamilton, K., Tidmarsh, G. F., De Young, L. R. and Lampidis, T. J. (2004) 2-Deoxy-D-glucose increases the efficacy of adriamycin and paclitaxel in human osteosarcoma and non-small cell lung cancers *in vivo*. Cancer Res. **64**, 31–34

26 Lampidis, T. J., Bernal, S. D., Summerhayes, I. C. and Chen, L. B. (1993) Selective toxicity of rhodamine 123 in carcinoma cells *in vitro*. Cancer Res. **43**, 716–720

27 Kurtoglu, M. and Lampidis, T. J. (2009) From delocalized lipophilic cations to hypoxia: blocking tumor cell mitochondrial function leads to therapeutic gain with glycolytic inhibitors. Mol. Nutr. Food Res. **53**, 68–75

28 Filomeni, G., Cerchiaro, G., Da Costa Ferreira, A. M., De Martino, A., Pedersen, J. Z., Rotilio, G. and Ciriolo, M. R. (2007) Pro-apoptotic activity of novel isatin–Schiff base copper(II) complexes depends on oxidative stress induction and organelle-selective damage. J. Biol. Chem. **282**, 12010–12021

Received 21 March 2011/4 May 2011; accepted 6 May 2011
Published as BJ Immediate Publication 6 May 2011, doi:10.1042/BJ20110510

29 Filomeni, G., Piccirillo, S., Graziani, I., Cardaci, S., Da Costa Ferreira, A. M., Rotilio, G. and Ciriolo, M. R. (2009) The isatin–Schiff base copper(II) complex [Cu(isaepy)$_2$] acts as delocalized lipophilic cation, yields widespread mitochondrial oxidative damage and induces AMP-activated protein kinase-dependent apoptosis. Carcinogenesis **30**, 1115–1124

30 Cerchiaro, G., Aquilano, K., Filomeni, G., Rotilio, G., Ciriolo, M. R. and Da Costa Ferreira, A. M. (2005) Isatin–Schiff base copper(II) complexes and their influence on cellular viability. J. Inorg. Biochem. **99**, 1433–1440

31 Riccardi, C. and Nicoletti, I. (2006) Analysis of apoptosis by propidium iodide staining and flow cytometry. Nat. Protoc. **1**, 1458–1461

32 Filomeni, G., Desideri, E., Cardaci, S., Graziani, I., Piccirillo, S., Rotilio, G. and Ciriolo, M. R. (2010) Carcinoma cells activate AMP-activated protein kinase-dependent autophagy as survival response to kaempferol-mediated energetic impairment. Autophagy **6**, 202–216

33 Cardaci, S., Filomeni, G., Rotilio, G. and Ciriolo, M. R. (2010) p38^{MAPK}/p53 signalling axis mediates neuronal apoptosis in response to tetrahydrobiopterin-induced oxidative stress and glucose uptake inhibition: implication for neurodegeneration. Biochem. J. **430**, 439–451

34 Lowry, O. H., Rosebrough, N. J., Farr, A. L. and Randall, R. J. (1951) Protein measurement with the Folin phenol reagent. J. Biol. Chem. **193**, 265–275

35 Xia, Y., Ongusaha, P., Lee, S. W. and Liou, Y. C. (2009) Loss of Wip1 sensitizes cells to stress- and DNA damage-induced apoptosis. J. Biol. Chem. **284**, 17428–17437

36 Reference deleted

37 Lee, Y. M., Lee, J. O., Jung, J. H., Kim, J. H., Park, S. H., Park, J. M., Kim, E. K., Suh, P. G. and Kim, H. S. (2008) Retinoic acid leads to cytoskeletal rearrangement through AMPK-Rac1 and stimulates glucose uptake through AMPK-p38^{MAPK} in skeletal muscle cells. J. Biol. Chem. **283**, 33969–33974

38 Geschwind, J. F., Ko, Y. H., Torbenson, M. S., Magee, C. and Pedersen, P. L. (2002) Novel therapy for liver cancer: direct intraarterial injection of a potent inhibitor of ATP production. Cancer Res. **62**, 3909–3913

39 Geschwind, J. F., Georgiades, C. S., Ko, Y. H. and Pedersen, P. L. (2004) Recently elucidated energy catabolism pathways provide opportunities for novel treatments in hepatocellular carcinoma. Expert Rev. Anticancer Ther. **4**, 449–457

40 Ko, Y. H., Pedersen, P. L. and Geschwind, J. F. (2001) Glucose catabolism in the rabbit VX2 model for liver cancer. Cancer Lett. **173**, 83–91

41 Pereira da Silva, A. P., El-Bacha, T., Kyaw, N., dos Santos, R. S., da Silva, W. S., Almeida, F. C., Da Poian, A. T. and Galina, A. (2009) Inhibition of energy-producing pathways of HepG2 cells by 3-bromopyruvate. Biochem. J. **417**, 717–726

42 Herrero-Mendez, A., Almeida, A., Fernández, E., Maestre, C., Moncada, S. and Bolaños, J. P. (2009) The bioenergetic and antioxidant status of neurons is controlled by continuous degradation of a key glycolytic enzyme by APC/C-Cdh1. Nat. Cell Biol. **11**, 747–752

43 Tennant, D. A., Durán, R. V. and Gottlieb, E. (2010) Targeting metabolic transformation for cancer therapy. Nat. Rev. Cancer **10**, 267–277

44 Acan, N. L. and Ozer, N. (2001) Modification of human erythrocyte pyruvate kinase by an active site-directed reagent: bromopyruvate. J. Enzyme Inhib. **16**, 457–464

45 Baker, J. P. and Rabin, B. R. (1969) Effects of bromopyruvate on the control and catalytic properties of glutamate dehydrogenase. Eur. J. Biochem. **11**, 154–159

46 Ganapathy-Kanniappan, S., Vali, M., Kunjithapatham, R., Buijs, M., Syed, L. H., Rao, P. P., Ota, S., Kwak, B. K., Loffroy, R. and Geschwind, J. F. (2010) 3-Bromopyruvate: a new targeted antiglycolytic agent and a promise for cancer therapy. Curr. Pharm. Biotechnol. **11**, 510–517

47 Ganapathy-Kanniappan, S., Geschwind, J. F., Kunjithapatham, R., Buijs, M., Vossen, J. A., Tchernyshyov, I., Cole, R. N., Syed, L. H., Rao, P. P., Ota, S. and Vali, M. (2009) Glyceraldehyde-3-phosphate dehydrogenase (GAPDH) is pyruvylated during 3-bromopyruvate mediated cancer cell death. Anticancer Res. **29**, 4909–4918

48 Kim, J. S., Ahn, K. J., Kim, J. A., Kim, H. M., Lee, J. D., Lee, J. M., Kim, S. J. and Park, J. H. (2008) Role of reactive oxygen species-mediated mitochondrial dysregulation in 3-bromopyruvate induced cell death in hepatoma cells: ROS-mediated cell death by 3-BrPA. J. Bioenerg. Biomembr. **40**, 607–618

49 Chen, Z., Zhang, H., Lu, W. and Huang, P. (2009) Role of mitochondria-associated hexokinase II in cancer cell death induced by 3-bromopyruvate. Biochim. Biophys. Acta **1787**, 553–560

Biochem. J. (2011) **437**, 443–453 (Printed in Great Britain) doi:10.1042/BJ20110510

SUPPLEMENTARY ONLINE DATA

Metabolic oxidative stress elicited by the copper(II) complex [Cu(isaepy)$_2$] triggers apoptosis in SH-SY5Y cells through the induction of the AMP-activated protein kinase/p38^{MAPK}/p53 signalling axis: evidence for a combined use with 3-bromopyruvate in neuroblastoma treatment

Giuseppe FILOMENI*[1], Simone CARDACI*[1], Ana Maria DA COSTA FERREIRA†, Giuseppe ROTILIO*‡ and Maria Rosa CIRIOLO*‡[2]

*Department of Biology, University of Rome "Tor Vergata", via della Ricerca Scientifica, 00133 Rome, Italy, †Departamento de Química Fundamental, Instituto de Química, Universidade de São Paulo, Av. Prof. Lineu Prestes 748, CEP 05508-900, São Paulo, SP, Brazil, and ‡Research Centre IRCCS San Raffaele Pisana, Via dei Bonacolsi, 00163 Rome, Italy

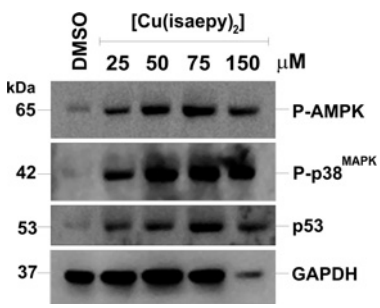

Figure S1 Dose–dependent effects of [Cu(isaepy)2] on phospho-AMPK, phospho-p38^{MAPK} and p53 in SH-SY5Y cells

SH-SY5Y cells were treated with different concentrations of [Cu(isaepy)$_2$] (25, 50, 75 and 150 μM) or, as a control, with equal volumes of DMSO. At the indicated times, 30 μg of total protein extract was loaded on to each lane for the detection of basal and phospho-activated levels of AMPK and p38^{MAPK}, as well as p53. GAPDH was used as a loading control. Western blots are from one experiment and are representative of three that gave similar results. Molecular-mass markers are shown on the left.

Received 21 March 2011/4 May 2011; accepted 6 May 2011
Published as BJ Immediate Publication 6 May 2011, doi:10.1042/BJ20110510

[1] These authors contributed equally to the study.
[2] To whom correspondence should be addressed (email ciriolo@bio.uniroma2.it).